Controlled Growth of Zinc Oxide Nanowire Arrays by Chemical Vapor Deposition (CVD) Method

Waseem A. Bhutto[1], Abdul Majid Soomro[1], Altaf H. Nizamani[1], Hussain Saleem[2*], Murad Ali Khaskheli[1], Ali Ghulam Sahito[3], Roshan Das[1], Usman Ali Khan[1], Samina Saleem[2,4]

[1]Institute of Physics, University of Sindh, Jamshoro, Pakistan.
[2]Department of Computer Science, UBIT, University of Karachi, Karachi, Pakistan.
[3]Centre for Pure & Applied Geology, University of Sindh, Jamshoro, Pakistan.
[4]Karachi University Business School, KUBS, University of Karachi, Pakistan.
*Corresponding Author: hussainsaleem@uok.edu.pk

Abstract
The Nanostructured materials like nanotubes, nanowires, nanorods, and nanobelts etc. have remained the subject of interest these days because of its unique thermal, mechanical and optical properties. Zinc Oxide (ZnO), is the most attractive material due to its unique properties and availability of a variety of growth methods. At nanostructured level, the properties of ZnO can be altered by controlling the growth process, such as the shape, size, morphology, aspect ratio and density control. In this work, Aligned ZnO Nanowires (NWs) were successfully synthesized by Chemical Vapor Deposition (CVD) on Aluminum doped Zinc Oxide (AZO) substrate. The effects of different growth parameters such as growth temperature, flow rate of oxygen and distance of substrate from source on growth of aligned ZnO NWs have been investigated and discussed in detail. Morphologies and structures of grown nanowire arrays were characterized by Scanning Electron Microscopy (SEM) and X-ray diffraction (XRD). Optical properties were optimized by UV-visible transmittance spectra, and photo luminescence (PL).

Key words:
Chemical Vapor Deposition; Controlled Growth; Nano Structure; Nanotubes; Nanowire Arrays; Optics;

1. Introduction

The nanostructure materials are currently the most popular research targets because of their relatively high surface area to volume ratio, high crystallinity, great stoichiometry, and low impurity concentrations [1][2][3][4]. Zinc Oxide (ZnO), in its nanostructured form, is the most appealing material because of its direct band gap of $3.37\ eV$ and high exciton binding energy of $60\ meV$. Recently, $1D$, $2D$ and $3D$ nanostructures, which show a diversity of morphologies, such as nanowires (NWs), nanorods (NRs), nanobelts, and nanotubes, have received increasing attention due to their unique physical properties, which differ from bulk materials, especially nanowires (NWs) can provide effective conduction paths for electrons [5][6] due to their high crystallinity compared to a thin-film structure which makes it suitable for applications in photovoltaic, electrical, piezoelectric, opto-electrical and electrochemical devices, such as ultraviolet (UV) sensors [7], photodetectors [8], Light-Emitting Diodes (LED) [9], solar cells [10], photo sensors [11], Resistive-switching Random Access Memory (RRAM) [12][13], nano-generators [14][15], nano-capacitors [16], and gas sensors [17][18].

The performance of ZnO based devices strongly depend on their dimensions and morphologies [19][20][21][22][23][24][25][26]. Therefore, the investigation of ZnO nano-structures in highly oriented, aligned and ordered arrays is of critical importance for the development of novel devices. Different methods have been used to synthesize ZnO nanowire arrays, such as metal organic CVD, laser ablation and solution phase method. Most of them are expensive or environmentally un-attractive [27][28][29]. In this work, we synthesize the ZnO nanowires by CVD method to overcome these issues. In order to achieve vertically well aligned ZnO nanowires, different parameters have been adapted, including growth temperature, flow rate of oxygen and distance of substrate from source. Morphologies, structures and optical properties were characterized by scanning electron microscopy (SEM), X-ray diffraction (XRD), UV-visible transmittance spectra, and photo luminescence (PL).

2. Experimental Procedure

There are many possible methods to synthesize ZnO nano-materials, however, the observed properties depend mainly on the preparation conditions. Since we know that the substrate material has a significant effect on the morphology of ZnO nanowires [30]. Therefore, it is convenient to use ZnO thin layer as a seed layer for nucleation of nanowires growth. In this work, we prepared the substrate using transparent conductive glass coated with an aluminum zinc oxide (AZO) layer, which have high electrical conductivity and optical transmittance value. The growth of vertically well-aligned ZnO nanowire arrays on AZO substrate was carried out in a horizontal quartz tube furnace with three heating zones. Zinc powder ($5N, 1g$) was used as the source material and placed at the central heating zone of the quartz tube. Three pieces of AZO substrate with the dimensions of ($1\ cm \times 1\ cm$) were placed at a distance of $7{\sim}9\ cm$ downstream of the Zn powder. Before heating, the system

Manuscript received August 5, 2019
Manuscript revised August 20, 2019

Table-1. The Growth Parameters of ZnO Nanowire Arrays. Variations in Growth Temperature ($°C$).

S. No	Zn (g)	O_2, N_2 Flow ($sccm$)	Distance between Source and Substrate (cm)	Growth Temp ($°C$)
1	1.0	10,100	8	540
2	1.0	10,100	8	560
3	1.0	10,100	8	580

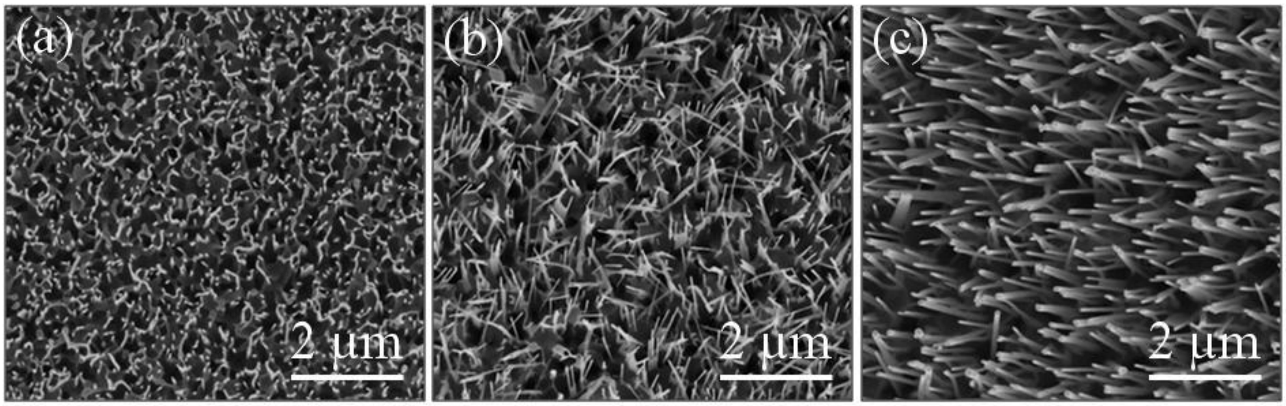

Fig.1. SEM images of ZnO nanowire arrays at different temperatures: (a) $540\ °C$; (b) $560\ °C$; (c) $580\ °C$. Variations in Growth Temp ($°C$).

was evacuated to $1.0 \times 10^{-2}\ Pa$, and a mixed gas consisting of $100\ sccm$ N_2 flow and $8{\sim}10\ sccm$ O_2 flow was introduced into the tube. Abbreviation $sccm$ stands for "standard cubic centimeters per minute" [34]. Then, the tube was heated to $540°C{\sim}580°C$ at a rate of $20°C/min$ and maintained at this temperature for 30 min[35][36][37][38].

The diameter and density of nanowires were controlled by the distance between substrate and source. After the growth, the tube furnace was cooled down to room temperature.

3. Results and Discussion

3.1 Effect of Growth Temperature on ZnO Nanowire Arrays

In CVD process, morphology and the structure of a final product can be controlled by the temperature and the level of super-saturation. Generally, for the growth of nanowire arrays, the growth direction and rate are two important factors which determine whether a nanowire can be formed. However, the growth rate mainly depends on the growth temperature [31]. In order to study the effect of temperature on ZnO nanowire arrays, we used three different temperatures i.e. $540°C$, $560°C$ and $580°C$. The growth parameters are illustrated in Table-1, and the morphologies of these samples were analyzed by SEM shown in Fig.1.

It has been noticed that the Zn source evaporated very little at the low growth temperature of $540°C$, which causes the low Zn vapor pressure. Insufficient Zn vapor pressure slows down the growth rate along all directions [32]. As a result, the final product is very short ZnO nanowires or even a layer of ZnO thin film, as shown in Fig.1(a). Increasing the temperature to $560°C$, leads to grow random nanowires, as depicted in Fig.1(b). Further increasing the temperature at $580°C$, the more evaporation of the Zn source occurs and reacts with oxygen. Due to high temperature Zn and O vapors with high kinetic energy diffuse much more easily to form the ZnO nanowires and make the orientation of nanowires better, as shown in Fig.1(c). From the Fig.1, it can be seen that as the temperature rises, the average diameter of nanowires is gradually increased, because the higher ZnO vapor pressure leads to larger ZnO seeds during initial growth [39][40][41][42].

3.2 Effect of Oxygen Flow Rate on ZnO Nanowire Arrays

In order to study the effect of oxygen flow on the growth of ZnO nanowires, we used different flow rates as 8 $sccm$, 9 $sccm$ and 10 $sccm$ oxygen flows. Growth parameters are listed in Table-2, and the SEM images are shown in Fig.2. From the figure we can see that well aligned nanowires were grown for these three parameters, and in this case, the oxygen flow has little effect on the diameter and relatively density. As we know, nanowire diameter and density are

Table-2. The Growth Parameters of ZnO Nanowire Arrays. Variations in O_2, N_2 Flow ($sccm$).

S. No	Zn (g)	O_2, N_2 Flow ($sccm$)	Distance between Source and Substrate (cm)	Growth Temp ($°C$)
1	1.0	8,100	8	580
2	1.0	9,100	8	580
3	1.0	10,100	8	580

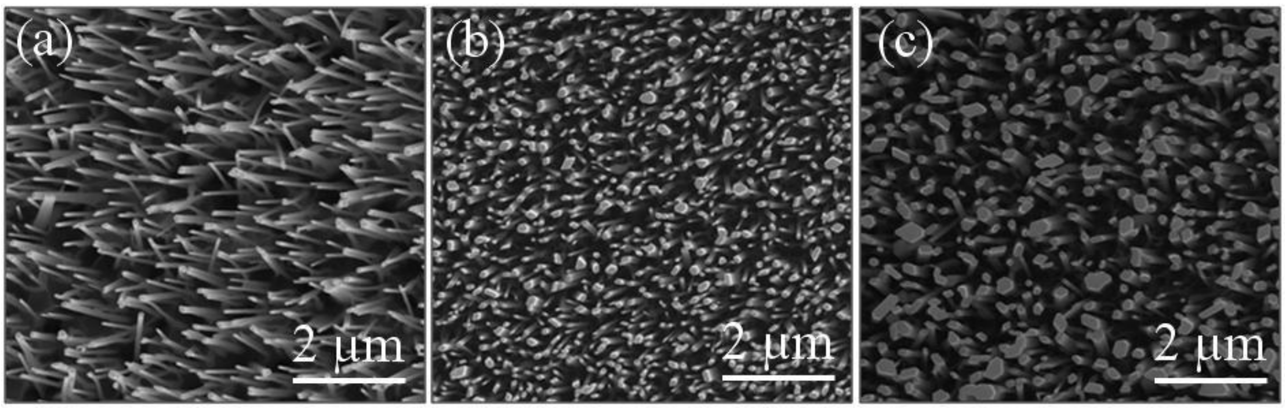

Fig.2. SEM images of ZnO nanowire arrays with different oxygen concentration, (a) 8%, (b) 9%, (c) 10%. Variations in O_2, N_2 Flow ($sccm$).

crucial for coating the shell layer on ZnO nanowires. If the density is too high or the diameter is too large, it will be difficult to deposit a shell layer around the entire ZnO nanowires. For low density or small diameter, the shell deposition is easier but it reduces light absorption which degrades the efficiency of device. By changing the flow rate we can control the density of nanowires, and can get a favorable condition for the growth of coaxial nanowires.

In our experiments, we also tried lower and the higher oxygen flow rate, but it has been found that when the oxygen flow is too high or too low, the nanowires look disorganized and therefore not listed here [33][43][44][45].

3.3 Effect of Zn Vapor Pressure on ZnO Nanowire Arrays

As we already discussed, Zn vapor pressure increases by increasing the growth temperature. At low temperature, the Zn vapor pressure was low, which resulted in short nanowires, while at high temperature Zn vapor pressure was high enough, which cause a gradual increase in diameter. Furthermore, different distances of the substrate away from the source also affect the Zn vapor pressure. To study the effect of distance from source on the ZnO nanowires growth, we used different substrate positions at 7 cm, 8 cm and 9 cm away from the Zn source. The growth parameters are given in Table-3. The SEM images of samples can be seen in Fig.3. When we put substrate at 7 cm close to Zn source, the Zn vapor pressure increases; thus enhance the super saturation level. The high vapor pressure can promote growth in several directions, which results in the formation of clusters as shown in Fig.3 (a). The increase of 8 cm distance away from source decreases the Zn vapor pressure. At lower Zn vapor pressure, nanowire arrays preferably grow in good orientation as shown in Fig.3 (b). Further little increase in position of substrate at 9 cm, the density of nanowires is decreased as shown in Fig.3 (c). From above experiments, we conclude that 8 cm distance is relatively better than 9 cm distance for suitable growth of nanowires.

4. Characterization of ZnO Nanowire Arrays

From the above different experiments, we conclude that the growth parameters for well-aligned ZnO nanowires were used as 1.0 g of high-purity Zn powder, N_2 flow rate of 100 $sccm$, O_2 flow rate of 8 $sccm$, growth temperature 580$°C$ and the substrate position 8 cm away from source material.

4.1 Morphology

To further analyze the surface morphology of ZnO nanowire arrays, we conduct SEM measurements for these samples. Aligned ZnO nanowire arrays are found to be synthesized on the c-oriented AZO substrate. The top view of aligned ZnO nanowire arrays is demonstrating the high growth

Table-3. The Growth Parameters of ZnO Nanowire Arrays. Variations in (cm) distance between source and substrate.

S. No	Zn (g)	O_2, N_2 Flow ($sccm$)	Distance between Source and Substrate (cm)	Growth Temp (°C)
1	1.0	8,100	7	580
2	1.0	8,100	8	580
3	1.0	8,100	9	580

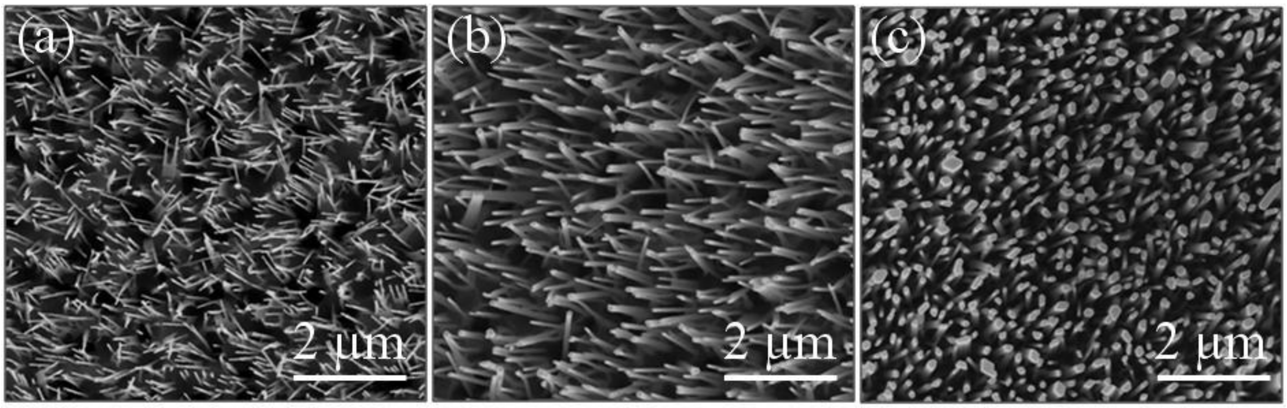

Fig.3. SEM images of ZnO nanowire arrays at different substrate positions, (a) 7 cm, (b) 8 cm, and (c) 9 cm. Variations in (cm) distance between source and substrate.

density, as shown in Fig.4 (a). It is also observed that the nanowires are hexagonal in crystal structure, and are preferentially oriented in the c-axis direction. Fig.4 (b) shows the cross-sectional view of ZnO nanowire arrays, illustrating that the length of the synthesized nanowire arrays is about $3\mu m$ and their diameters vary from 20 to 250 nm.

4.2 Material Structures

Under general conditions, ZnO is single crystalline and exhibits a hexagonal wurtzite structure. Fig.5 shows the XRD pattern of ZnO nanowire arrays. In particular, we can see that only one diffraction peak appears at $2\theta = 34.68°$, corresponding to wurtzite structure of ZnO (002) with d-spacing of 0.26 nm. The sharp (002) peak confirms that ZnO nanowires have grown along their c-axis perpendicular to the substrate with good crystalline quality. To avoid the influence of the substrate, measurements were taken at $5°$ grazing angle.

4.3 Optical Properties

To observe the optical properties of ZnO nanowire arrays, we performed PL and UV-visible transmittance measurements. Fig.6 shows the PL spectrum of ZnO nanowire arrays measured at room temperature.

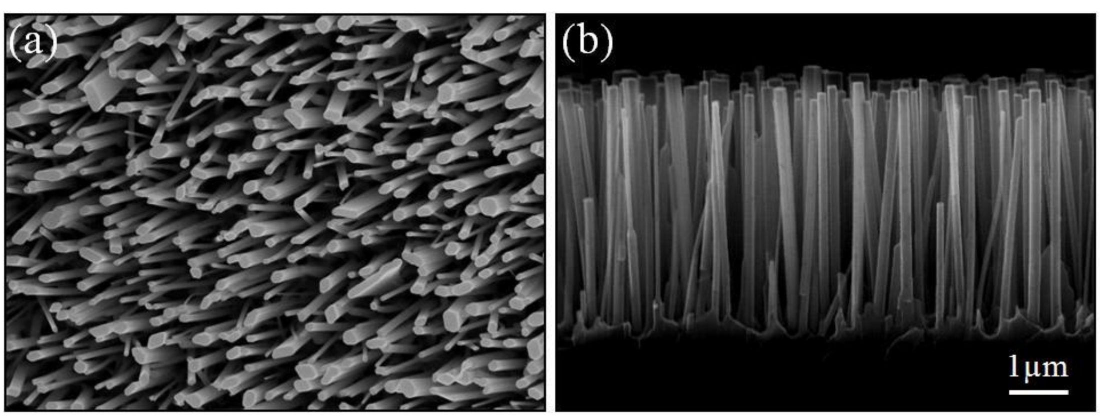

Fig.4. SEM images of ZnO nanowire arrays (a) top view, (b) cross-sectional view.

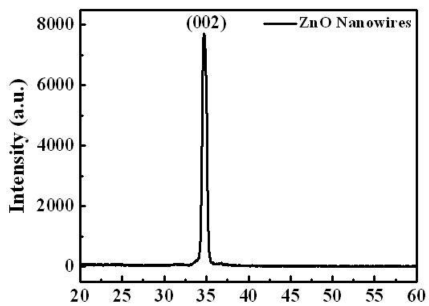

2 Theta (deg.); $2\theta = 34.68°$

Fig.5. XRD pattern of ZnO nanowire arrays.

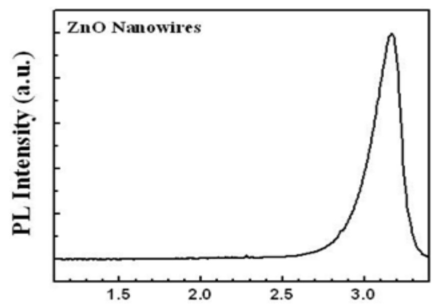

Energy (eV); $E_g = 3.2\ eV$

Fig.6. PL spectrum of ZnO nanowire arrays.

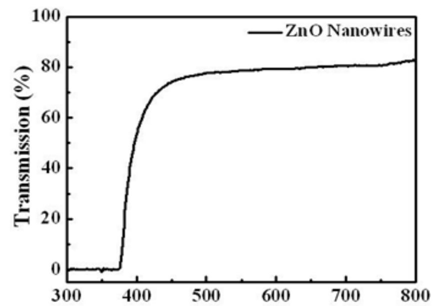

Wavelength (nm);

Fig.7. Transmission spectrum of ZnO nanowire arrays.

Only a strong UV emission peak was observed at $380\ nm$ ($E_g = 3.2\ eV$). This UV emission is understood as near-band-edge (NBE) emission [34].

No other emission peak was observed, indicating the good crystal quality of ZnO nanowire arrays.

The UV-visible transmittance curve of ZnO nanowire arrays is given in Fig.7. The absorption onset is around $400\ nm$, which corresponds to a band gap of $3.2\ eV$, indicating that ZnO nanowire arrays absorb light only in the ultraviolet region. While at longer wavelength, there is no absorption; the curve looks very flat in visible region, indicating that nanowires have good crystal quality.

The transmittance reaches to 0 when the wavelength is below $380\ nm$, indicating the ZnO nanowire arrays have high absorption coefficient [46][47][48][49][50].

5. Conclusions

In summary, well aligned ZnO nanowire arrays have been synthesized by CVD. Different parameters, such as growth temperature, oxygen flow rate, and Zn vapor pressure, have been modified to obtain the suitable conditions for aligned ZnO nanowire arrays.

We used high-purity Zn powder of $1.0\ g$, N_2 flow rate of $100\ sccm$, O_2 flow rate of $8\ sccm$, chamber pressure at $10\ Pa$, growth temperature $580°C$, 30 minutes growth time, $8\ cm$ distance between substrate and Zn source for achieving the vertical nanowire arrays on AZO substrate. SEM and XRD have been used to investigate their morphologies, structures and optical properties, respectively.

Characterization results show the preferential growth of ZnO nanowire arrays with wurtzite structure along (001) direction. Finally, PL spectrum and UV-visible transmittance spectrum demonstrate the good crystal quality of ZnO nanowire arrays.

References

[1] Wang, Y., et al., Facile fabrication of reduced graphene oxide covered $ZnCo_2O_4$ porous nanowire array hierarchical structure on Ni-foam as a high performance anode for a lithium-ion battery. RSC Advances, 2016. 6(1): p. 547-554.

[2] Jiang, H., J. Ma, and C. Li, Hierarchical porous $NiCo_2O_4$ nanowires for high-rate supercapacitors. Chemical Communications, 2012. 48(37): p. 4465-4467.

[3] Yin, J., et al., NiO/CoN Porous Nanowires as Efficient Bifunctional Catalysts for Zn–Air Batteries. ACS Nano, 2017. 11(2): p. 2275-2283.

[4] Han, Y., et al., Porous SnO_2 nanowire bundles for photocatalyst and Li ion battery applications. CrystEngComm, 2011. 13(10): p. 3506-3510.

[5] Cheng, B. and E.T. Samulski, Hydrothermal synthesis of one-dimensional ZnO nanostructures with different aspect ratios. Chemical Communications, 2004(8): p. 986-987.

[6] Wang, Z.L., Ten years' venturing in ZnO nanostructures: from discovery to scientific understanding and to technology applications. Chinese Science Bulletin, 2009. 54(22): p. 4021.

[7] Ho, J.-H., et al., Observing Solid-State Formation of Oriented Porous Functional Oxide Nanowire Heterostructures by in Situ TEM. Nano Letters, 2018. 18(9): p. 6064-6070.

[8] Soci, C., et al., ZnO Nanowire UV Photodetectors with High Internal Gain. Nano Letters, 2007. 7(4): p. 1003-1009.

[9] Lee, W.-C., et al., Phosphorus-Doped p–n Homojunction ZnO Nanowires: Growth Kinetics in Liquid and Their Optoelectronic Properties. Chemistry of Materials, 2015. 27(12): p. 4216-4221.

[10] Wu, Y.-T., et al., Nickel/Platinum Dual Silicide Axial Nanowire Heterostructures with Excellent Photosensor Applications. Nano Letters, 2016. 16(2): p. 1086-1091.

[11] Huang, C.-W., et al., Revealing Controllable Nanowire Transformation through Cationic Exchange for RRAM Application. Nano Letters, 2014. 14(5): p. 2759-2763.

[12] Chang, Y.-T., et al., Excellent piezoelectric and electrical properties of lithium-doped ZnO nanowires for nanogenerator applications. Nano Energy, 2014. 8: p. 291-296.

[13] Hong, Y.-S., et al., Single-crystalline CuO nanowires for resistive random access memory applications. Applied Physics Letters, 2015. 106(17): p. 173103.

[14] Tsai, T.-C., et al., In Situ TEM Investigation of the Electrochemical Behavior in CNTs/MnO_2-Based Energy Storage Devices. Analytical Chemistry, 2017. 89(18): p. 9671-9675.

[15] Wang, Z.L. and J. Song, Piezoelectric Nanogenerators Based on Zinc Oxide Nanowire Arrays. Science, 2006. 312(5771): p. 242.

[16] Ahn, M.W., et al., Gas sensing properties of defect-controlled ZnO-nanowire gas sensor. Applied Physics Letters, 2008. 93(26): p. 263103.

[17] Wan, Q., et al., Fabrication and ethanol sensing characteristics of ZnO nanowire gas sensors. Applied Physics Letters, 2004. 84(18): p. 3654-3656.

[18] Ma, G. and X. Wang, Synthesis and Applications of One-Dimensional Porous Nanowire Arrays: A Review. Nano, 2014. 10(01): p. 153000

[19] Wang, Z., Zinc oxide nanostructures: growth, properties and applications. J. Phys.: Condens. Matter, 2004. 16: p. 829-858.

[20] Leung, Y.H., et al., Zinc oxide ribbon and comb structures: synthesis and optical properties. Chemical Physics Letters, 2004. 394(4): p. 452-457.

[21] Wang, X., et al., Controllable ZnO Architectures by Ethanolamine-Assisted Hydrothermal Reaction for Enhanced Photocatalytic Activity. The Journal of Physical Chemistry C, 2011. 115(6): p. 2769-2775.

[22] Mo, M., et al., Self-Assembly of ZnO Nanorods and Nanosheets into Hollow Microhemispheres and Microspheres. Advanced Materials, 2005. 17(6): p. 756-760.

[23] Gu, Z., et al., Aligned ZnO Nanorod Arrays Grown Directly on Zinc Foils and Zinc Spheres by a Low-Temperature Oxidization Method. ACS Nano, 2009. 3(2): p. 273-278.

[24] Gao, P.X., et al., Conversion of Zinc Oxide Nanobelts into Superlattice-Structured Nanohelices. Science, 2005. 309(5741): p. 1700-1704.

[25] Sun, T., J. Qiu, and C. Liang, Controllable Fabrication and Photocatalytic Activity of ZnO Nanobelt Arrays. The Journal of Physical Chemistry C, 2008. 112(3): p. 715-721.

[26] Kong, X., et al., Single-Crystal Nanorings Formed by Epitaxial Self-Coiling of Polar Nanobelts. Science (New York, N.Y.), 2004. 303: p. 1348-51.

[27] Kayes, B.M., H.A. Atwater, and N.S. Lewis, Comparison of the device physics principles of planar and radial p-n junction nanorod solar cells. Journal of Applied Physics, 2005. 97(11): p. 114302.

[28] Tian, B., et al., Coaxial Silicon Nanowires as Solar Cells and Nanoelectronic Power Sources. Nature, 2007. 449: p. 885-9.

[29] Zhang, Y., L.-W. Wang, and A. Mascarenhas, "Quantum Coaxial Cables" for Solar Energy Harvesting. Nano letters, 2007. 7: p. 1264-9.

[30] Greene, L.E., et al., General Route to Vertical ZnO Nanowire Arrays Using Textured ZnO Seeds. Nano Letters, 2005. 5(7): p. 1231-1236.

[31] Ye, Z.Z., et al., Catalyst-free MOCVD growth of aligned ZnO nanotip arrays on silicon substrate with controlled tip shape. Solid State Communications, 2007. 141: p. 464-466.

[32] Zeng, J.H., et al., High-density arrays of low-defect-concentration zinc oxide nanowire grown on transparent conducting oxide glass substrate by chemical vapor deposition. Acta Materialia - ACTA MATER, 2009. 57: p. 1813-1820.

[33] H. Wan and H. Ruda, A study of the growth mechanism of CVD-grown ZnO Nanowires [J]. Journal of Materials Science: Materials in Electronics, 2010. 21(10): 1014-1019. Wan, H. and H. Ruda, A study of the growth mechanism of CVD-grown ZnO nanowires. Journal of Materials Science: Materials in Electronics, 2010. 21: p. 1014-1019.

[34] Kong, Y.C., et al., Ultraviolet-emitting ZnO nanowires synthesized by a physical vapor deposition approach. Applied Physics Letters, 2001. 78(4): p. 407-409.

[35] Wu, Zhiming, et al. "An all-inorganic type-II heterojunction array with nearly full solar spectral response based on ZnO/ZnSe core/shell nanowires." Journal of Materials Chemistry 21.16, 2011. p. 6020-6026.

[36] M. Y. Channa, A. H. Nizamani, H. Saleem, W. A. Bhutto, A. M. Soomro, and M. Y. Soomro, "Surface Ion Trap Designs for Vertical Ion Shuttling," IJCSNS International Journal of Computer Science and Network Security, 2019. vol. 19, no. 4.

[37] H. Saleem, A. H. Nizamani, W. A. Bhutto, A. M. Soomro, M. Y. Soomro, A. Toufik, "Two Dimensional Natural Convection Heat Losses from Square Solar Cavity Receiver," IJCSNS International Journal of Computer Science and Network Security, 2019. vol. 19, no. 4.

[38] A. M. Soomro, W. A. Bhutto, A. H. Nizamani, H. Saleem, M. Y. Soomro, M. A. Khaskheli, N. M. Shaikh, "Controllable Growth of Hexagonal BN Monolayer Sheets on Cu Foil by LPCVD," IJCSNS International Journal of Computer Science and Network Security, 2019. vol. 19, no. 6.

[39] R. Chand, Saeeduddin, M. A. Khaskheli, A. M. Soomro, H. Saleem, W. A. Bhutto, A. H. Nizamani, M.Y. Soomro, N. M. Shaikh, S. V. Muniandy, "Fractal Analysis of Light Scattering Data from Gravity-Driven Granular Flows," IJCSNS International Journal of Computer Science and Network Security, 2019. vol. 19, no. 7.

[40] M. Y. Channa, A. H. Nizamani, A. M. Soomro, H. Saleem, W. A. Bhutto, M. Y. Soomro, M. A. Khaskheli, N. M. Shaikh, "Vertical Ion Shuttling Protocols for Multi-Strip Surface Ion Traps," IJCSNS International Journal of Computer Science and Network Security, 2019. vol. 19, no. 7.

[41] S. Jamali, W. A. Bhutto, A. H. Nizamani, H. Saleem, M. A. Khaskheli, A. M. Soomro, A. G. Sahito, N. M. Shaikh, S. Saleem, "Spectroscopic Analysis of Lithium Fluoride (LiF)

using Laser Ablation," IJCSNS International Journal of Computer Science and Network Security, 2019. vol. 19, no. 8.

[42] A. H. Nizamani, B. Rasool, M. Tahir, N. M. Shaikh, H. Saleem, “Adiabatic ION Shuttling Protocols in Outer-Segmented-Electrode Surface ION Traps,” International Journal of Scientific & Engineering Research (IJSER), 2013. 4(6), 3055-3061.

[43] A. H. Nizamani, S. A. Buzdar, B. Rasool, N. M. Shaikh, H. Saleem, Computer-based frequency drift control of multiple LASERs in real-time. International Journal of Scientific & Engineering Research (IJSER), 2013. 4(6), 3038.

[44] A. H. Nizamani, M. A. Rind, N. M. Shaikh, A. H. Moghal, H. Saleem, Versatile Ultra High Vacuum System for ION Trap Experiments: Design and Implementation. Intl. Journal of Advancements in Research & Technology, USA, 2013. 2(5).

[45] S. A. Buzdar, M. A. Khan, A. Nazir, M. A. Gadhi, A. H. Nizamani, H. Saleem, Effect of Change in Orientation of Enhanced Dynamic Wedges on Radiotherapy Treatment Dose. IJoART, 2013. 2, 496-500.

[46] H. Saleem & et al., "Imposing Software Traceability and Configuration Management for Change Tolerance in Software Production," IJCSNS International Journal of Computer Science and Network Security, 2019. vol. 19, no. 1.

[47] H. Saleem & et al., "Novel Intelligent Electronic Booking Framework for E-Business with Distributed Computing and Data Mining," IJCSNS International Journal of Computer Science and Network Security, 2019. vol. 19, no. 4.

[48] H. Saleem & et al., “Data Science and Machine Learning Approach to Improve E-Commerce Sales Performance on Social Web," IJCSNS International Journal of Computer Science and Network Security, 2019. vol. 19, no. 9.

[49] H. Saleem & et al., “Behavioral Tendency Analysis towards E-Participation for Voting in Political Elections using Social Web," IJCSNS International Journal of Computer Science and Network Security, 2019. vol. 19, no. 9.

[50] H. Saleem & et al., “Review of Various Aspects of Radio Frequency IDentification (RFID) Technology,” International Organization for Scientific Research - Journal of Computer Engineering (IOSR-JCE), 2012. vol. 8, no. 1.